Photoinduced Electron-Transfer, Pyrolyses, and Direct Irradiation Reactions of 2-Methylenecyclobutanones: Regioselective Bond Cleavage Depends on the Substituents and the Method of Activation

Hiroshi Ikeda,*[a] Futoshi Tanaka,[a] Tsutomu Miyashi,[a] Kimio Akiyama,[b] and Shozo Tero-Kubota[b]

Keywords: Bond cleavage / Electron transfer / Methylenecyclobutanone / Photochemistry / Regioselectivity

The regioselectivity of bond cleavage and the subsequent reactivity of 4-methylene-3,3-dimethyl-2,2-diphenylcyclobutan-1-one (**5**) and 4-isopropylidene-2,2-diphenylcyclobutan-1-one (**6**) in photoinduced electron transfer, pyrolysis, and direct irradiation reactions were investigated. Novel photoinduced electron-transfer rearrangements of **5** and **6** were found to occur through 1,4-diyl radical cations formed by C1–C2 cleavage of $\mathbf{5}^{\cdot+}$ and $\mathbf{6}^{\cdot+}$; that is, similarly to radical-cation Norrish type I cleavage, but in contrast to the diansyl derivative $\mathbf{1}^{\cdot+}$ corresponding to $\mathbf{5}^{\cdot+}$, which gives an oxatetramethyleneethane (OTME)-type radical cation through C2–C3 cleavage. In contrast, solvent effects on the thermal rearrangement of **5** to **6** and theoretical calculations suggested the intervention of an OTME-type diradical intermediate $\mathbf{16}^{\cdot\cdot}$ formed by homolytic C2–C3 cleavage of **5**. In direct photoreactions, **5** and **6** undergo [2+2] cycloreversion to give 1,1-diphenylethylenes and methyleneallenes, which are explained by both C1–C2 and C3–C4 cleavage. Consequently, the regioselectivity of **5** and **6** in bond cleavage and their reactivity strongly depend on the substituents and the method of activation.

Introduction

2-Methylenecyclobutan-1-one (MCB) is a unique compound that readily participates in a variety of reactions (Scheme 1). If a strained C2−C3 bond cleaves either homolytically or heterolytically, MCB will give an oxa-analogue of tetramethyleneethane[1,2] − oxatetramethyleneethane (OTME, 3-methylenebutan-2-one-1,4-diyl) − which is a new substance in the field of non-Kekulé chemistry. The chemical properties of OTME are of great interest because replacement of a carbon atom with an oxygen atom in a non-Kekulé molecule induces considerable changes in the geometry, multiplicity, electronic structure, and reactivity of the compound, as exemplified by the oxyallyl,[3] oxa-analogue of trimethylenemethane.[4,5] Moreover, if both C1−C2 and C3−C4 cleave, MCB may participate in a metathesis-type reaction, since MCB is obtained through a [2+2] cycloaddition (making C1−C4 and C2−C3 bonds) between an allene and a ketene. Consequently, we studied the regioselectivity of bond cleavage of dianisyl derivatives of MCB − 4-methylene-3,3-dimethyl-2,2-bis(4-methoxyphenyl)cyclobutan-1-one (**1**) and 4-isopropylidene-2,2-bis(4-methoxyphenyl)cyclobutan-1-one (**2**) − under photoinduced electron-transfer (PET) conditions with *p*-chloranil (CA) as a sensitizer (Scheme 2).[6] Substrate **1** undergoes re-

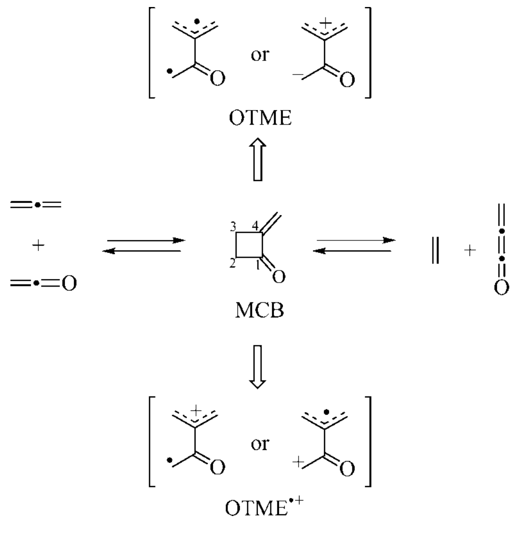

Scheme 1. Possible reaction pathways of MCB

---

[a] Department of Chemistry, Graduate School of Science, Tohoku University,
Sendai 980−8578, Japan
Fax: (internat.) +81-22-217-6557
E-mail: ikeda@org.chem.tohoku.ac.jp
[b] Institute of Multidisciplinary Research for Advanced Materials, Tohoku University,
Sendai 980−8577, Japan
Fax: (internat.) +81-22-217-5612
E-mail: akiyama@tagen.tohoku.ac.jp

Supporting information for this article is available on the WWW under http://www.eurjoc.org or from the author.

arrangement to give **2** via an OTME-type radical cation intermediate ($3^{\cdot+}$) formed by C2−C3 cleavage of $1^{\cdot+}$, whereas the C1−C2 bond of $2^{\cdot+}$ cleaves to give a CA adduct **4**.

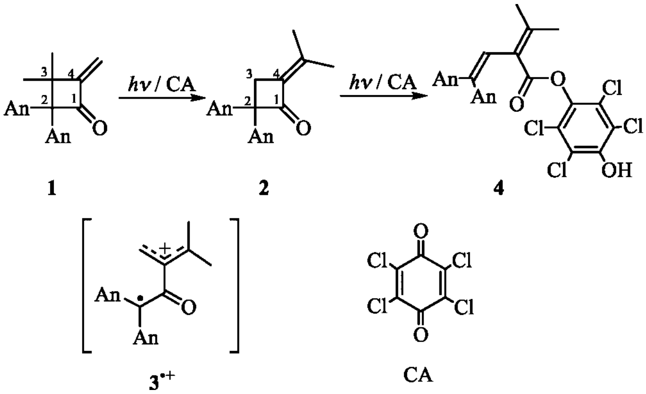

Scheme 2. PET reactions of **1** and **2** with CA; An = 4-MeOC$_6$H$_4$

To gain further insight into the regioselective bond cleavage and reactivity of MCB, we also studied the PET reactions of 4-methylene-3,3-dimethyl-2,2-diphenylcyclobutan-1-one (**5**)[7] and 4-isopropylidene-2,2-diphenylcyclobutan-1-one (**6**,[7] Scheme 3), as well as pyrolyses and direct irradiation reactions. Unlike the PET reaction of dianisyl derivative **1**, those of **5** and **6** involved C1−C2 cleavage. It appeared that a diradical type of OTME derivative was intervening in the thermal rearrangement of **5**, while a zwitterionic counterpart rather than the diradical was proposed as the intermediate in the rearrangement from **5** to **6**.[7] Direct photo-irradiation of **5** and **6** resulted in a half metathesis-type reaction accompanied by C1−C2 and C3−C4 cleavage. Here we report the unique reactivity of **5** and **6**, the bond cleavage regioselectivities of which depend strongly on the substituents and the method of activation (Scheme 3).

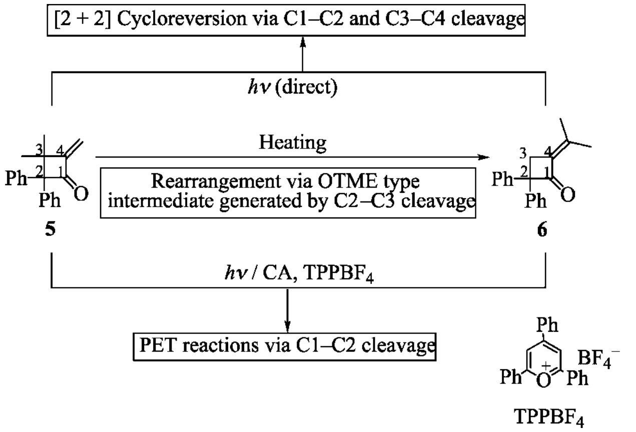

Scheme 3. Regioselective bond cleavage of **5** and **6** depends on the substituent and the method of activation

Results and Discussion

PET Reactions of 5 and 6

MCB derivatives **5** and **6** were prepared by thermal [2+2] cycloaddition between 1,1-dimethylallene and diphenylketene according to the method reported by Brook and coworkers.[7] The halfwave oxidation potentials (E_p^{ox}) of **5** and **6** are low enough to quench the excited states of CA and triphenylpyrylium tetrafluoroborate (TPPBF$_4$) exergonically, as suggested by the calculated free energy changes (ΔG_{et}) for electron transfer.[8−10] In agreement with calculations, **5** efficiently quenches TPPBF$_4$ fluorescence in aerated acetonitrile and dichloromethane. Table 1 shows the values of E_p^{ox}, ΔG_{et}, and the rate constants (k_q) for the TPPBF$_4$-fluorescence quenching by **5** and **6**.

Compound **5** was consumed with 43% conversion on irradiation ($\lambda > 400$ nm) in the presence of CA for 60 min in degassed dichloromethane, but no obvious product was observed. In contrast, TPPBF$_4$-sensitized photo-irradiation of **5** for 10 min in dichloromethane produced a mixture of the isomers 3,4-dihydro-3,3-dimethyl-2-methylene-4-phenyl-2*H*-naphthalen-1-one (**7**, Scheme 4) and 2,3,4-trimethyl-4-phenyl-4*H*-naphthalen-1-one (**8**), in 28 and 24% yields, respectively, at 69% conversion. Similar PET reactions of **5** to give **7** and **8** took place in the more polar acetonitrile, although the yields were lower, as shown in Table 2. Control photo-irradiation of **7** for 10 min in dichloromethane resulted in the quantitative recovery of **7**. Similar photo-irradiation of **6** afforded completely different results. A CA adduct, 2′,3′,5′,6′-tetrachloro-4′-hydroxyphenyl 2-isopropylidene-4,4-diphenyl-3-butenoate (**9**), was formed in CA-sensitized photo-irradiation of **6** in dichloromethane (59% yields at 59% conversion). In contrast, TPPBF$_4$-sensitized photo-irradiation of **6** in dichloromethane or acetonitrile gave a rearranged isomer of 3,4-dihydro-2-isopropylidene-

Table 1. Oxidation potentials (E_p^{ox}) of **5** and **6**, free energy changes (ΔG_{et}) associated with electron-transfer reactions of **5** and **6** with CA* or TPPBF$_4$* in CH$_3$CN or CH$_2$Cl$_2$, and the quenching rate constants (k_q) for TPPBF$_4$*

	E_p^{ox}[a] [V]		ΔG_{et}(CA)[b] [eV]		ΔG_{et}(TPPBF$_4$)[b] [eV]		k_q [10^{10} M^{-1} s^{-1}]	
	CH$_3$CN	CH$_2$Cl$_2$	CH$_3$CN	CH$_2$Cl$_2$	CH$_3$CN	CH$_2$Cl$_2$	CH$_3$CN	CH$_2$Cl$_2$
5	+2.05	+2.13	[c]	−0.94	−0.46	−0.74	1.6	1.5
6	+1.87	+1.89	[c]	−1.18	−0.64	−0.98	1.9	2.0

[a] Vs. SCE in CH$_3$CN containing 0.1 M Et$_4$NClO$_4$, or in CH$_2$Cl$_2$ containing 0.1 M nBu$_4$NBF$_4$, irreversible. [b] ΔGet = [E^{ox}_p (**5** or **6**) − 0.03] − $E^{red}_{1/2}$(sensitizer) − E_{0-0}(sensitizer) + c. $E^{red}_{1/2}$(TPPBF$_4$) = −0.39 V, E_{0-0}(TPPBF$_4$) = 2.87 eV, c = 0.00 eV in CH$_3$CN. $E^{red}_{1/2}$(CA) = +0.12 V, E_{0-0}(CA) = 2.69 eV, $E^{red}_{1/2}$(TPPBF$_4$) = −0.20 V, E_{0-0}(TPPBF$_4$) = 2.81 eV, c = −0.23 eV in CH$_2$Cl$_2$. [c] No attempt.

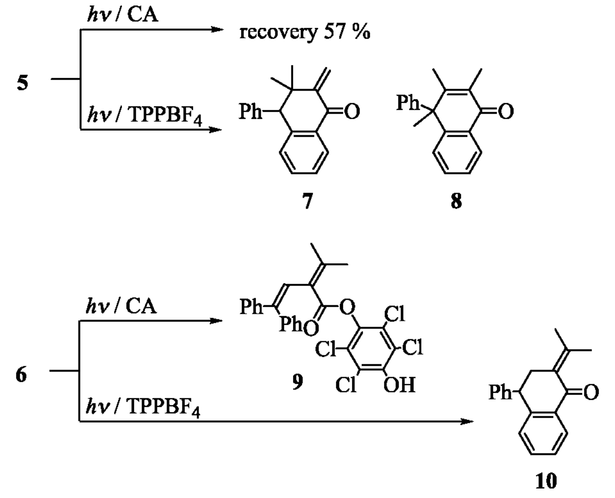

Scheme 4. PET reactions of **5** and **6** with CA or $TPPBF_4$

Table 2. PET reactions of **5** and **6** under various sets of conditions

[a]			Time [min]	Conversion [%]	Yields [%]			
	Sensitizer	Solvent			7	8	9	10
5	CA	CH_2Cl_2	60	43	0	0	0	0
	$TPPBF_4$	CH_2Cl_2	5	32[b]	19	9	0	0
			10	69[b]	28	24	0	0
		CH_3CN	5	34	11	3	0	0
			10	64	21	5	0	0
6	CA	CH_2Cl_2	5	30	0	0	30	0
			10	59	0	0	59	0
	$TPPBF_4$	CH_2Cl_2	2	51	0	0	0	44
			5	92	0	0	0	54
		CH_3CN	5	63	0	0	0	59
			10	93	0	0	0	81

[a] [**5** or **6**] = [CA] = 0.01 M, [$TPPBF_4$] = 0.003 M. [b] A small amount (5–6%) of 3-methylene-4,4-dimethyl-5,5-diphenyltetrahydrofuran-2-one (**23**) was also formed during the reactions.

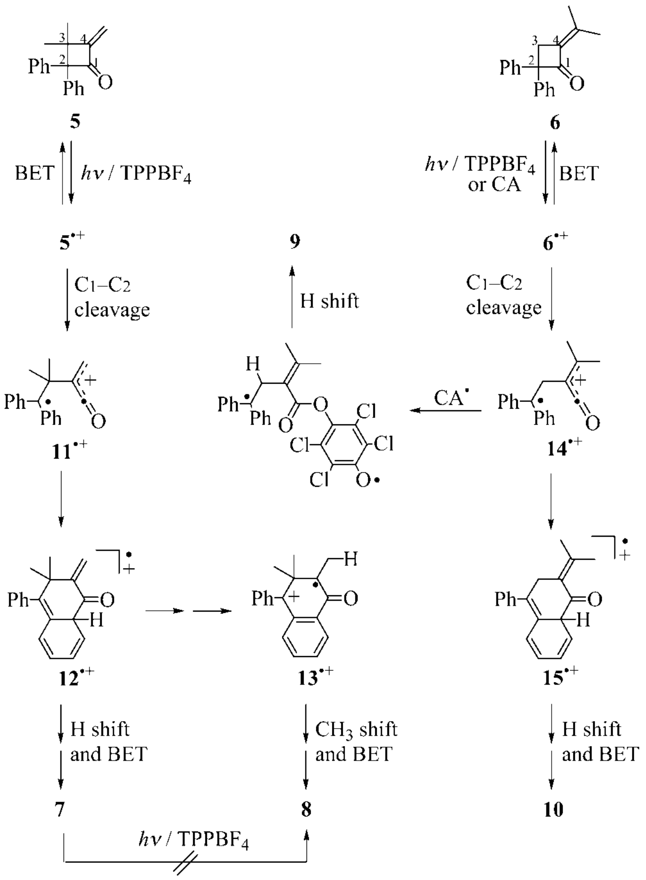

Scheme 5. A plausible mechanism for PET reactions of **5** and **6** in the presence of CA or $TPPBF_4$

4-phenyl-2*H*-naphthalen-1-one (**10**) in moderate to good yield.

Scheme 5 shows a plausible reaction mechanism for the $TPPBF_4$- or CA-sensitized PET reactions of **5** and **6**. The initially formed $\mathbf{5}^{\cdot+}$ undergoes C1−C2 cleavage to give $\mathbf{11}^{\cdot+}$, which undergoes subsequent cyclization to form a fused radical cation, $\mathbf{12}^{\cdot+}$. Ketone **7** is formed from $\mathbf{12}^{\cdot+}$ though a formal 1,7-H shift and back electron transfer (BET) from the triphenylpyranyl radical, whereas **8** is the result of a 1,2-CH_3 shift and BET in the 1,3-radical cation $\mathbf{13}^{\cdot+}$, which is probably formed from $\mathbf{12}^{\cdot+}$. In fact, a large difference between $\mathbf{12}^{\cdot+}$ and $\mathbf{13}^{\cdot+}$ in their calculated heats of formation suggests a facile rearrangement of $\mathbf{12}^{\cdot+}$ to $\mathbf{13}^{\cdot+}$.[11] The high stability of **7** shown in the control experiment excludes the possible conversion of **7** to **8**. A similar mechanism operates in the photoreaction of **6**. The initially formed $\mathbf{6}^{\cdot+}$ also undergoes C1−C2 cleavage to give $\mathbf{14}^{\cdot+}$. In the case of CA sensitization, the reaction between $\mathbf{14}^{\cdot+}$ and $CA^{\cdot-}$ involves a sequence of additions and a formal H shift to give the CA adduct **9**. For $TPPBF_4$ sensitization, ketone **10** is formed from $\mathbf{15}^{\cdot+}$ through an H shift and BET, as with ketone **7**. The C1−C2 cleavage of $\mathbf{5}^{\cdot+}$ and $\mathbf{6}^{\cdot+}$ is similar to radical-cation Norrish type I cleavage, as reported for arylalkyl ketones by Akaba and co-workers (Scheme 6)[12] and as exemplified by the dianisyl derivatives **2** (Scheme 2).[6]

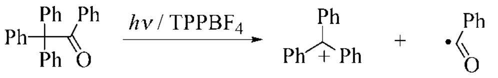

Scheme 6. The first example of a radical-cation Norrish type I reaction

Two electronic structures are possible for key intermediates $\mathbf{11}^{\cdot+}$ and $\mathbf{14}^{\cdot+}$, as shown in Figure 1 (a) with the parent framework: type A has formal ethyl radical and ketoallyl cation subunits, while type B possesses ethyl cation and ketoallyl radical subunits. The electronic and stereochemical structures of $\mathbf{11}^{\cdot+}$ and $\mathbf{14}^{\cdot+}$ shown in Scheme 5 are supported by PM5/UHF−AM1/UHF calculations. As shown in Figure 1 (b) and Table 3, $\mathbf{11}^{\cdot+}$ prefers a twisted structure for Type A with dihedral angles of $\alpha \approx +46°$, $\beta \approx +5°$, and $\gamma = +3°$. The sum of the calculated partial spin density ($\Sigma\rho = +0.99$) of the ethyl (actually 2-methyl-1,1-diphenylpropyl) subunit of $\mathbf{11}^{\cdot+}$ is markedly higher than that of the ketoallyl subunit. Accordingly, the sum of the calculated partial charge density ($\Sigma q = +0.72$) of the ketoallyl subunit is higher than the value for the ethyl subunit. This is also the case with **14**$^{\cdot+}$. A similar theoretical calculation suggested that type A of **14**$^{\cdot+}$ with the 1,1-diphenylethyl radical and the 3,3-dimethylketoallyl cation subunits has a twisted structure (Figure 1, b).[13]

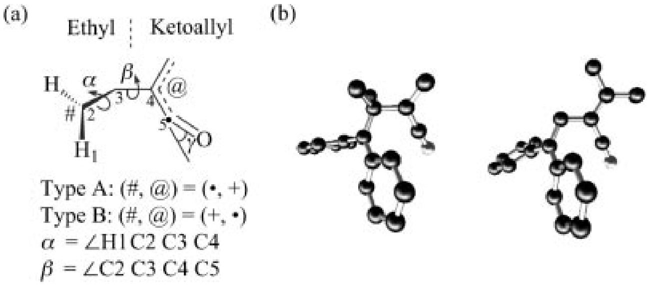

Figure 1. (a) Definition of the dihedral angles (α, β, and γ) and two subunits in the parent framework; (b) geometries of **11**$^{\cdot+}$ and **14**$^{\cdot+}$ (hydrogen atoms are omitted for clarity) optimized by PM5/UHF

Substituent Effects on the Regioselectivity of Bond Cleavage in 1$^{\cdot+}$ and 5$^{\cdot+}$

As described above, the dianisyl derivative **1** undergoes rearrangement to **2** via **3**$^{\cdot+}$, which is formed by C2−C3 bond cleavage (Scheme 2). The difference in bond cleavage regioselectivities between the dianisyl and diphenyl derivatives **1**$^{\cdot+}$ and **5**$^{\cdot+}$ is an intriguing feature in the PET reactions (Scheme 7). Miranda and co-workers recently reported similar substituent effects on regioselectivity in the bond cleavage of diaryl-substituted oxetane radical cations (Scheme 8).[14−16] They suggested that an anisyl group decreases the strength of the C2−C3 σ bond through a σ−π interaction to stabilize the positive charge of the aromatic radical cation. This is not the case in our system, however, because the diarylmethyl subunits probably possess spin, as described above, regardless of the structures of **3**$^{\cdot+}$ and **11**$^{\cdot+}$.

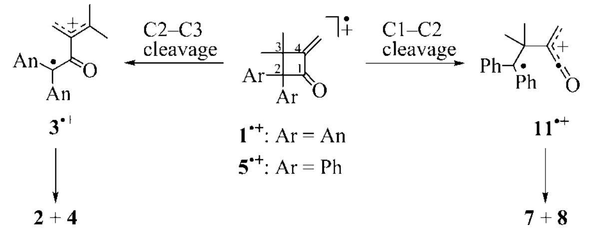

Scheme 7. Contrasting regioselectivities in the bond cleavage of **1**$^{\cdot+}$ and **5**$^{\cdot+}$

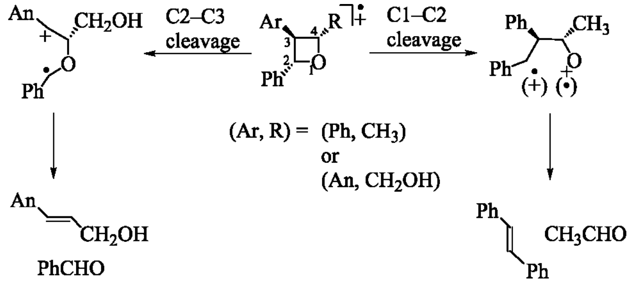

Scheme 8. Contrasting regioselectivities in the bond cleavage of diaryl-substituted oxetane radical cations

To gain further insight into the substituent effects on the regioselectivity, we conducted B3LYP/6−31G(d,p) calculations for **1** and **5**. As shown in Figure 2, the HOMO of **1** is located mainly on the two anisyl subunits. Conversely, the two phenyl groups, the C1−C2 and C1−C4 bonds, and the carbonyl subunit are all associated with the HOMO in **5**. The driving force of the C2−C3 cleavage in **1**$^{\cdot+}$, analogously to the thermal rearrangement of **1**, must be a relaxation of the steric repulsion between the two pairs of anisyl and methyl groups in the eclipsed conformation. Similar steric repulsion between the two pairs of phenyl and methyl groups would be expected for **5**$^{\cdot+}$, but the considerable distribution of the HOMO into the C1−C2 bond induces its cleavage after oxidation by single electron transfer. Note that oxidation hardly affects the steric repulsion in **5**$^{\cdot+}$, while the C1−C2 bond order is readily affected. The substitution on the phenyl ring strongly affects their balance and consequently the regioselectivity of the radical-cation bond cleavage.

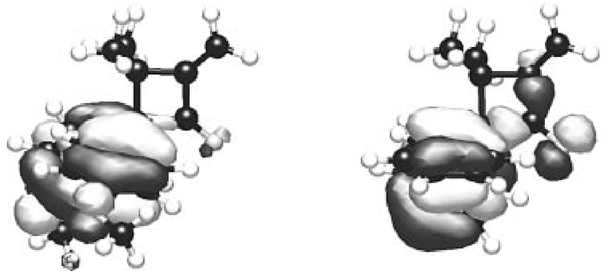

Figure 2. The HOMOs of **1** (dianisyl, left) and **5** (diphenyl, right) obtained by B3LYP/6−31G(d,p) calculations

Table 3. Dihedral angles (α, β, and γ), the sum of calculated partial spin and charge densities (Σρ and Σ*q*), and types of electronic structures of **11**$^{\cdot+}$ and **14**$^{\cdot+}$ calculated by PM5/UHF−AM1/UHF

Radical cation	α [°]	β [°]	γ [°]	Σρ Ethyl	Ketoallyl	Σ*q* Ethyl	Ketoallyl	Type
11$^{\cdot+}$	+46.3	+5.1	+3.0	+0.99	+0.01	+0.28	+0.72	A
14$^{\cdot+}$	+36.4	+18.4	+5.0	+0.98	+0.02	+0.24	+0.76	A

Thermal Rearrangement of 5 to 6 via an OTME Intermediate

Brook and co-workers also found[7] that the rate constant for the rearrangement of **5** increases by less than twofold when the solvent is changed from *o*-dichlorobenzene [DCB, $E_T(30)$[17] = 38.0 kcal·mol^{-1}] to benzonitrile [$E_T(30)$ = 41.5 kcal·mol^{-1}]. They assumed the generation of a zwitterionic OTME-type intermediate **16**$^{+-}$ formed by heterolytic C2−C3 cleavage rather than the formation of an alternative OTME-type diradical counterpart **16**$^{\cdot\cdot}$ generated by homolytic C2−C3 cleavage, and concluded that the observed solvent effects are not inconsistent with this assumption (Scheme 9).

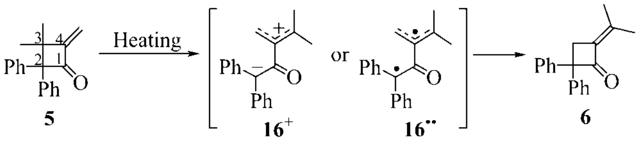

Scheme 9. Two possible intermediates (**16**$^{+-}$ and **16**$^{\cdot\cdot}$) in the thermal rearrangement of **5**

In contrast, calculations suggest that **16**$^{\cdot\cdot}$ is preferable to **16**$^{+-}$ regardless of the method (AM1 or PM5) or medium (in vacuo or in DMSO with ε = 45). As judged from the sums of the calculated partial spin and charge densities (Σρ and Σ*q*, respectively, in Table 4), **16** has a pair of spins at the 1,1-dimethylallyl and the diphenylmethyl subunits and no significant charge anywhere, suggesting a contribution from the diradical **16**$^{\cdot\cdot}$. Figure 3 (b) shows a doubly twisted structure of **16** with dihedral angles of θ ≈ +53° and ω ≈ +63°, optimized by AM1/UHF calculation. The diphenylmethyl and the carbonyl subunits are both twisted with respect to each other, as in the case with the carbonyl and the 1,1-dimethylallyl subunits. The large deviation from a planar structure is probably due to the radical stabilizing effects of the two phenyl groups and steric hindrance between the phenyl and the dimethylallyl groups in **16** with a hypothetical planar structure.

The appropriate electronic structure of **16** is indicated by solvent and substituent effects observed in reinvestigation of the thermal rearrangement of **1** and **5** in the 110−140 °C range in [D$_4$]DCB and [D$_6$]DMSO [$E_T(30)$ = 45.1 kcal·mol^{-1}], which is more polar than benzonitrile. The kinetic parameters are summarized in Table 5, together with those of Brook and co-workers.[7] No significant change in

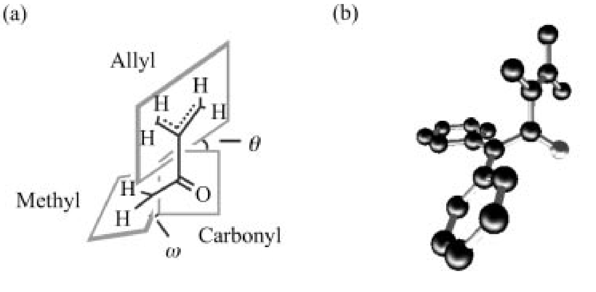

Figure 3. (a) Definition of the dihedral angles (θ and ω) and three subunits in the OTME framework; (b) the optimized geometry of **16** (hydrogen atoms are omitted for clarity) by AM1/UHF with ε = 45 for DMSO

Table 4. Dihedral angles (θ and ω), the sums of partial spin and charge densities (Σρ and Σ*q*), and types of electronic structures of **16**

Methods	ε	θ [°]	ω [°]	Σρ Allyl	Carbonyl	Methyl	Σ*q* Allyl	Carbonyl	Methyl	Type
AM1/UHF	0	+40.0	+85.6	+0.97	+0.08	−1.06	+0.00	+0.03	−0.04	**16**$^{\cdot\cdot}$
	45	+53.3	+63.4	+0.97	+0.07	−1.05	+0.00	+0.03	−0.03	**16**$^{\cdot\cdot}$
PM5/UHF	0	+45.3	+36.4	[a]	[a]	[a]	+0.00	+0.01	−0.02	**16**$^{\cdot\cdot}$
	45	+48.6	+36.7	[a]	[a]	[a]	+0.07	−0.12	+0.05	**16**$^{\cdot\cdot}$

[a] Not available.

Table 5. Kinetic parameters for thermal rearrangement of **1** and **5** at 130 °C

	Solvents	$E_T(30)$ [kcal·mol^{-1}]	E_a [kcal·mol^{-1}]	log A	k_{iso} [s^{-1}]	$\Delta G^{\ddagger}$ [kcal·mol^{-1}]	$\Delta H^{\ddagger}$ [kcal· mol^{-1}]	$\Delta S^{\ddagger}$ [cal·mol^{-1}·K^{-1}]
1	[D$_6$]DMSO	45.1	32.1	13.6	1.8×10^{-4}	30.8	31.3	1.3
	[D$_6$]DMSO/[D$_4$]DCB[a]	41.3	31.2	13.2	1.8×10^{-4}	30.8	30.4	−0.83
	[D$_4$]DCB	38.1	30.1	12.6	1.7×10^{-4}	30.8	29.3	−3.7
5	[D$_6$]DMSO	45.1	31.4	12.7	4.4×10^{-5}	31.9	30.6	−3.3
	[D$_4$]DCB	38.1	32.2	13.1	5.2×10^{-5}	31.8	31.4	−1.0
	[D$_4$]DCB[b]	38.1	33.3[b]	13.8[b]	5.2×10^{-5}[c]	31.7[c]	32.5[c]	1.9[c]

[a] A mixture of [D$_4$]DCB and [D$_6$]DMSO in a 4:1 ratio. [b] See ref.[7]. [c] Calculated values using kinetic data cited in ref.[7].

$\Delta G^{\ddagger}$ was observed in either **1** or **5** on changing the solvent. Furthermore, on comparison of **1** and **5**, the methoxy substitution on the two phenyl groups reduced $\Delta G^{\ddagger}$ by 1 kcal mol^{-1}. These results suggest that the transition structure of the reaction is a diradical $\mathbf{16}^{\cdot\cdot}$ rather than a zwitterion $\mathbf{16}^{+-}$, in accordance with the calculations. Note that if the contribution of $\mathbf{16}^{+-}$ is exclusive, the methoxy substitution on the two phenyl groups should increase $\Delta G^{\ddagger}$ considerably.

Direct Irradiation Reactions of 5 and 6

On irradiation ($\lambda > 350$ nm) of **5** in benzene, 2-methyl-1,1-diphenylpropene (**17**) was formed quantitatively (Scheme 10, Table 6). The expected counterpart, methyleneketene (**18**) was not detected during the reaction. Interestingly, however, unidentified polymeric materials formed in the reaction mixture. In contrast, the similar photoreaction of **6** gave 1,1-diphenylethylene (**19**) and 3,3-dimethylacrylic anhydride (**20**)[18] in 68 and 16% yields at 82% conversion. The structure of **20** was confirmed by comparison with an authentic sample prepared independently from 3,3-dimethylacrylic acid (**21**) and the corresponding chloride. As shown in Scheme 10, **20** is probably formed through the reaction of the expected counterpart isopropylideneketene (**22**) and **21**, which is probably formed by the hydrolysis of **22** with a trace amount of water remaining in the reaction system. The mechanism was confirmed by control experiments in H_2O- or D_2O-saturated benzene. The photoreaction of **6** in H_2O-saturated benzene gave **19** and **20**, in 86 and 58% yields, respectively. Note that the yield of **20** increased from 16 to 58% when the solvent was changed to H_2O-saturated benzene. The similar photoreaction of **6** in D_2O-saturated benzene gave **19** and [D_2]**20** with 85% D incorporation, in 73 and 52% yields, respectively.

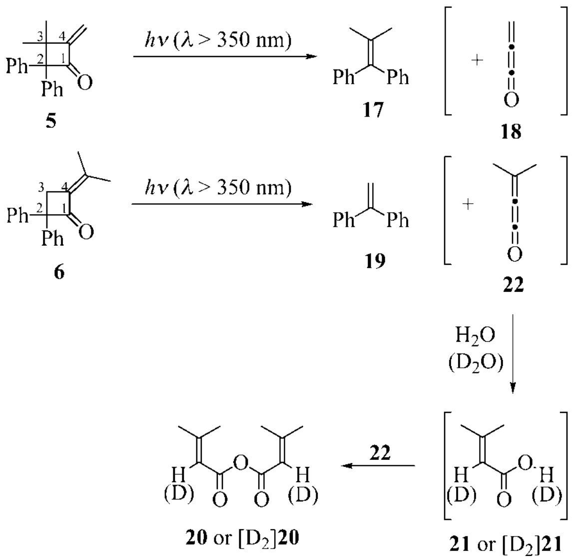

Scheme 10. Direct irradiation reactions of **5** and **6**

Table 6. Direct irradiation reactions of **5** and **6** for 6 h

[a]		Conversion [%]	Yields [%]		
	Solvents		**17**	**19**	**20** or [D_2]**20**
5	C_6H_6	52	50	–	–
6	C_6H_6	82	–	68	16
	H_2O-saturated C_6H_6	86	–	86	58
	D_2O-saturated C_6H_6	84	–	73	52 (D, 85%)

[a] [**5** or **6**] = 0.01 M.

Methyleneketenes are valuable synthetic intermediates and have attracted much mechanistic attention theoretically and experimentally.[19] In this connection, our photochemical [2+2] cycloreversion affording aliphatic methyleneketenes in situ at ambient temperature is quite useful in terms of synthetic organic chemistry, because methyleneketenes are typically generated by flash vacuum pyrolysis, irradiation of a low temperature matrix, or treatment of 2-bromoacryloyl chloride derivatives with some transition metal anion. Mazzocchi reported a similar photoreaction yielding aliphatic methyleneketenes for 3-isopropylidene-*N*-methyl-4,4-dimethylazetidin-2-one.[20]

Conclusion

We have found that the bond cleavage regioselectivities of **5** and **6** strongly depend on the method of activation (PET, pyrolysis, and direct irradiation) and the substitution on the parent framework and the phenyl groups. In PET reactions, we found a novel rearrangement of **5** and **6** via $\mathbf{11}^{\cdot+}$ and $\mathbf{14}^{\cdot+}$, which are formed by C1–C2 cleavage of $\mathbf{5}^{\cdot+}$ and $\mathbf{6}^{\cdot+}$, respectively. This is similar to a radical-cation Norrish type I cleavage,[6,12] but contrasts with the diansyl derivative $\mathbf{1}^{\cdot+}$, which gives an OTME-type radical cation $\mathbf{3}^{\cdot+}$ through C2–C3 cleavage.[6] Note that the regioselectivity of cyclobutane radical cations is a reaction of substantial biological importance because they are closely associated with UV damage and the photorepair of DNA.[21–25] Solvent effects and calculations suggested intervention by $\mathbf{16}^{\cdot\cdot}$ in the thermal rearrangement of **5**, which must be formed by hemolytic cleavage of the C2–C3 bond in **5**. In direct photoreactions, **5** and **6** gave 1,1-diphenylethylenes (**17** and **19**) and probably methyleneallenes (**18** and **22**), which were confirmed as **20** in the photoreaction of **6**. These reactions were explained in terms of [2+2] cycloreversions involving both C1–C2 and C3–C4 cleavage (Scheme 10). A formal metathesis reaction system (Schemes 1) was therefore demonstrated by the thermal cycloaddition of 1,1-dimethylallene with diphenylketene and photocycloreversion of **5** and **6** on direct irradiation.

Experimental Section

General Remarks: All melting and boiling points are uncorrected. Elemental analyses were performed by the Instrumental Analyses Center for Chemistry, Graduate School of Science, Tohoku University, and satisfactory elemental analyses were obtained for all the new compounds in this report. ^{1}H NMR spectra were recorded at 200 MHz with a Varian Gemini 2000 or at 400 MHz with a JEOL GX-400 spectrometer. Chemical shifts are reported with the following abbreviations: s, singlet; d, doublet; t, triplet; q, quadruplet; m, multiplet; br., broad; *J*, coupling constants (Hz). ^{1}H NMR product analyses were performed with the use of 1,1,2,2- or 1,1,1,2-tetrachloroethane as internal standards for integration. ^{13}C NMR spectra were obtained at 50 MHz with a Varian Gemini 2000 or at 100 MHz with a JEOL GX-400 spectrometer. Mass spectroscopy (MS) was performed with a JEOL JMS-HX110 or a Hitachi M-2500 mass spectrometer with electron or chemical ionization. The redox potentials (E_p^{ox} and E_p^{red} in V vs. SCE) were measured by cyclic voltammetry with a Yanaco P-1000 voltammetric analyzer or a PS-07 TOHO polarization unit in acetonitrile and dichloromethane containing Et_4NClO_4 (0.1 M) and nBu_4NBF_4 (0.1 M), respectively, as supporting electrolytes (Pt electrode, scan rate 100 mV/s). Since all of the substrates gave irreversible waves, their $E_{1/2}^{ox}$ values were estimated as $E_p^{ox} - 0.03$ V, a one-electron oxidation process being assumed. Fluorescence spectra were recorded on a Hitachi F-4010 fluorescence spectrophotometer. Steady-state photolysis was carried out at 20 ± 1 °C with an Ushio 2-kW Xe short arc lamp with an aqueous IR filter and a Toshiba cutoff filter L-39 ($\lambda > 360$ nm) for direct irradiation, or Y-43 ($\lambda > 400$ nm) for $TPPBF_4$- and CA-sensitization. The ethereal solvents were dried and distilled from $LiAlH_4$. Acetonitrile was dried and distilled from P_2O_5 and then $LiAlH_4$. Benzene and dichloromethane were dried and distilled from $LiAlH_4$. The deuterated solvents used for the kinetic study, [D$_6$]DCB (99.6% deuterated) and [D$_4$]DMSO (99.6%), were dried over 4 Å molecular sieves and treated with K_2CO_3 before use. Merck silica gel 60 (230−400 mesh) was used for column chromatography.

Preparation of 5 and 6: The two isomeric methylenecyclopropanes **5** and **6** were prepared in 8 and 30% yields, respectively, through a [2+2] cycloaddition between 3-methylbuta-1,2-diene (1,1-dimethylallene)[26] and diphenylketene,[27] by known procedures.[7]

Compound 5: Pale yellow cubes (*n*-hexane). M.p. 108−109 °C (ref.[7] 110.5 °C). IR (KBr): $\tilde{\nu}$ = 1744, 1651 cm^{-1} (ref.[7] 1739 cm^{-1}). MS (70 eV): *m*/*z* (%) = 262 (100) [M$^+$], 247 (31) [M$^+$ − CH$_3$], 219 (100) [247 − CO], 165 (6). ^{1}H NMR (200 MHz, CDCl$_3$): δ = 1.29 (s, 6 H), 5.12 (d, *J* = 1.1 Hz, 1 H), 5.88 (d, *J* = 1.1 Hz, 1 H), 7.20−7.44 (m, 10 H) ppm. ^{13}C NMR (50 MHz, CDCl$_3$): δ = 27.17 (2 C), 47.48, 77.95, 110.74 (2 C), 126.65 (2 C), 127.83 (4 C), 128.22 (4 C), 140.64, 162.38, 202.82 ppm.

Compound 6: Colorless plates (EtOH). M.p. 150−150.5 °C (ref.[7] 147 °C). IR (KBr): $\tilde{\nu}$ = 1724, 1663 cm^{-1} (ref.[7] 1720 cm^{-1}). MS (70 eV): *m*/*z* (%) = 262 (80) [M$^+$], 247 (10) [M$^+$ − CH$_3$], 219 (8) [M$^+$ − CO], 180 (100) [Ph$_2$C=C=CH$_2$]. ^{1}H NMR (200 MHz, CDCl$_3$): δ = 1.80 (s, 3 H), 2.15 (s, 3 H), 3.33 (br. s, 2 H), 7.15−7.45 (m, 10 H) ppm. ^{13}C NMR (50 MHz, CDCl$_3$): δ = 21.46, 21.59, 37.06, 70.20, 126.67 (2 C), 126.98 (4 C), 128.54 (4 C), 138.19, 142.79 (2 C), 145.83, 199.00 ppm.

General Procedure for TPPBF$_4$- or CA-Sensitized Photoreactions: A solution (6 mL) containing **5** or **6** (0.06 mmol) and TPPBF$_4$ (0.018 mmol) or CA (0.06 mmol) in a Pyrex test tube (diameter 1.5 cm) was degassed by five freeze−pump−thaw−cycles (−196 °C/10^{-2} Torr/ambient temperature) and was then sealed at 10^{-2} Torr. The sample solution was irradiated through a cutoff filter ($\lambda > 400$ nm) with a 2-kW Xe lamp at 20 ± 1 °C. For CA, the sample solution, which contained a slight suspension of CA, was irradiated similarly, after precipitation of CA by standing for 5 min. After evaporation in vacuo, the product yields were determined by ^{1}H NMR spectroscopy.

Isolation of 7, 8, and 10: A CH$_2$Cl$_2$ solution (18 mL) containing **5** (472 mg, 1.80 mmol) and TPPBF$_4$ (71.4 mg, 0.183 mmol) in a Pyrex test tube (diameter 2.5 cm) was degassed with five freeze−pump−thaw cycles (−196 °C/10^{-2} Torr/0 °C) and then sealed at 10^{-2} Torr. The sample solution was irradiated through a cutoff filter ($\lambda > 400$ nm) with a 2-kW Xe lamp at 20 ± 1 °C for 120 h. After evaporation in vacuo, column chromatography followed by recrystallization from hexane gave 109 mg (0.415 mmol, 23% yield) of **7**, 168 mg (0.639 mmol, 36%) of **8**, and 13.2 mg (0.0472 mmol, 3%) of **23**. A similar photoreaction of **6** (105 mg, 0.4 mmol) and TPPBF$_4$ (23.8 mg, 0.06 mmol) in CH$_3$CN (20 mL) for 2 h gave 57.9 mg (0.221 mmol, 55%) of **10**.

Compound 7: Yellow plates (*n*-hexane). M.p. 106−107 °C. IR (KBr): $\tilde{\nu}$ = 2968, 1668, 1595, 1454, 1272, 993, 947, 758 cm^{-1}. MS (EI, 70 eV): *m*/*z* (%) = 263 (20) [M$^+$ + 1], 262 (100) [M$^+$], 261 (10), 247 (18), 244 (32), 229 (13), 220 (16), 219 (16), 207 (15), 206 (16), 195 (13), 194 (33) [M$^+$ − (CH$_3$)$_2$C=C=CH$_2$], 171 (16), 166 (11), 165 (64), 91 (19, C$_7$H$_7$$^+$), 77 (50) [Ph$^+$]. ^{1}H NMR (400 MHz, CDCl$_3$): δ = 1.06 (s, 3 H), 1.25 (s, 3 H), 3.97 (s, 1 H), 5.28 (d, *J* = 1.6 Hz, 1 H), 6.33 (d, *J* = 1.6 Hz, 1 H), 6.96−6.99 (dd + m, *J* = 7.8, 1.8 Hz, 2 H), 7.13−7.19 (m, 4 H), 7.35 (ddd, *J* = 7.8, 7.8, 1.6 Hz, 1 H), 7.45 (ddd, *J* = 7.8, 7.8, 1.4 Hz, 1 H), 8.20 (dd, *J* = 7.8, 1.4 Hz, 1 H) ppm. ^{13}C NMR (100 MHz, CDCH$_3$): δ = 25.73, 30.54, 41.22, 58.57, 121.41, 126.66, 127.15, 127.79, 128.00 (2 C), 129.14 (2 C), 130.09, 131.69, 134.12, 141.05, 145.15, 150.00, 188.35 ppm.

Compound 8: Pale yellow plates (*n*-hexane). M.p. 112.5−113 °C. IR (KBr): $\tilde{\nu}$ = 1647, 1599, 1458, 1338, 773, 700, 709 cm^{-1}. MS (El, 70 eV): *m*/*z* (%) = 263 (20) [M$^+$ + 1], 262 (100) [M$^+$], 248 (12), 247 (61) [M$^+$ − CH$_3$], 232 (15), 229 (17), 219 (20) [M$^+$ − COCH$_3$], 204 (12), 203 (14), 202 (13), 159 (27). ^{1}H NMR (400 MHz, CDCl$_3$): δ = 1.74 (q, *J* = 2.0 Hz, 3 H), 1.82 (s, 3 H), 2.07 (q, *J* = 2.0 Hz, 3 H), 6.96 (ddd, *J* = 8.0, 1.6, 0.8 Hz, 1 H), 7.13−7.40 (m, 7 H), 8.21 (ddd, *J* = 8.0, 1.6, 0.8 Hz, 1 H) ppm. ^{13}C NMR (100 MHz, CDCl$_3$): δ = 11.7, 18.2, 27.1, 48.9, 126.3, 126.5, 126.7, 127.4 (2 C), 128.6 (2 C), 128.7, 129.5, 131.0, 132.0, 144.1, 150.8, 157.8, 184.3 ppm.

Compound 23: Colorless needles (*n*-hexane). M.p. 118.5−119.5 °C. IR (KBr): $\tilde{\nu}$ = 2982, 1759, 1300, 1211, 991, 763, 708 cm^{-1}. MS (EI, 70 eV): *m*/*z* (%) = 278 (16) [M$^+$], 105 (16) [C$_8$H$_9$$^+$ or PhCO$^+$], 96 (100) [M$^+$ − Ph$_2$CO], 77 (16) [Ph$^+$], 68 (65) [(CH$_3$)$_2$C=C=CH$_2$$^+$], 67 (12). ^{1}H NMR (400 MHz, CDCl$_3$): δ = 1.21 (s, 6 H), 5.46 (s, 1 H), 6.26 (s, 1 H), 7.27−7.49 (m, 10 H) ppm. ^{13}C NMR (100 MHz, CDCl$_3$): δ = 2.49 (2 C), 48.21, 92.63, 119.08, 126.75 (4 C), 127.77 (2 C), 128.06 (4 C), 140.21 (2 C), 147.08, 169.90 ppm.

Compound 10: Pale yellow powder (*n*-hexane). M.p. 56 °C. IR (KBr): $\tilde{\nu}$ = 1665, 1622, 1593, 1454, 1300, 1288, 1227, 708 cm^{-1}. MS (El, 70 eV): *m*/*z* (%) = 263 (20) [M$^+$ + 1], 262 (100) [M$^+$], 261 (8), 247 (18), 229 (8), 221 (5), 220 (9), 219 (8), 207 (10), 206 (11), 195 (9), 194 (14) [M$^+$ − (CH$_3$)$_2$C=C=CH$_2$], 178 (6), 171 (9), 165 (24), 115 (5), 91 (6, C$_7$H$_7$$^+$). ^{1}H NMR (200 MHz, CDCl$_3$): δ = 1.68 (s, 3 H), 2.17 (s, 3 H), 3.00 (dd, *J* = 13.7, 7.4 Hz, 1 H), 3.11 (dd, *J* = 13.7, 5.1 Hz, 1 H), 4.13 (dd, *J* = 7.4, 5.1 Hz, 1 H), 6.96 (dd, *J* = 6.4, 2.0 Hz, 1 H), 7.11 (*AA′BB′C*, *J* = 7.5, 2.0 Hz, 2 H), 7.20−7.42 (m, 5 H), 8.18 (dd, *J* = 6.8, 2.4 Hz, 1 H) ppm. ^{13}C NMR (50 MHz, CDCl$_3$): δ = 22.69, 23.17, 37.12, 46.07, 126.71, 127.10, 127.85, 128.41 (2 C +1 C), 128.48 (2 C), 128.83, 132.83, 134.99, 143.66, 145.41, 146.97, 189.97 ppm.

Isolation of 9: A CH$_2$Cl$_2$ solution (30 mL) containing **6** (78.7 mg, 0.3 mmol) and CA (80.4 mg, 0.33 mmol) in a Pyrex test tube (diameter 3.0 cm) was degassed with five freeze−pump−thaw cycles (−196 °C/10^{-2} Torr/ambient temperature) and then sealed at 10^{-2} Torr. After precipitation of CA by standing for 5 min, the sample solution was irradiated through a cutoff filter ($\lambda > 400$ nm) with a 2-kW Xe lamp at 20 ± 1 °C for 2 h. After evaporation in vacuo, column chromatography followed by recrystallization from acetone gave 91.2 mg (0.0179 mmol, 60% yield) of **9**.

Compound 9: Colorless powder. M.p. 219.5−220 °C. IR (KBr): $\tilde{\nu}$ = 3344, 1724, 1441, 1396, 1180, 1165, 1042, 764, 698 cm^{-1}. MS (CI, 15 eV): *m*/*z* (%) = 513 (12), 512 (13), 511 (51), 510 (26), 509 (100) [MH$^+$], 508 (20), 507 (75), 262 (7), 261 (31). ^{1}H NMR (200 MHz, [D$_6$]DMSO): δ = 0.69 (s, 3 H), 1.03 (s, 3 H), 1.55 (s, 1 H), 5.68 (br. s, 1 H), 6.20−6.50 (m, 10 H) ppm. ^{13}C NMR (50 MHz, [D$_6$]DMSO): δ = 22.49, 24.78, 120.97, 122.87, 123.63, 126.12, 127.97 (2 C), 128.09 (2 C), 128.29 (2 C), 128.54 (2 C), 128.72 (2 C), 129.70 (2 C), 137.76, 139.92, 142.26, 145.99, 149.72, 154.60, 163.42 ppm.

General Procedure used in the Kinetic Study: [D$_4$]DCB, [D$_6$]DMSO, and a mixture of both in 4:1 ratio were used for the kinetic study. A solution (0.6 mL) containing **5** (0.012 mmol, 0.02 M) in a Pyrex NMR tube (diameter 0.5 cm) was degassed with five freeze−pump−thaw cycles (−196 °C/10^{-2} Torr/ambient temperature) and then sealed at 10^{-2} Torr. The sample solution was heated in a controlled thermal bath. The relative and absolute yields of **6** were determined by ^{1}H NMR without and with an internal standard, respectively.

Direct Irradiation Reaction: A dehydrated or H_2O- or D_2O-saturated C_6H_6 solution (6 mL) containing **5** and **6** (15.7 mg, 0.06 mmol) in a Pyrex test tube (diameter 1.5 cm) was degassed with five freeze−pump−thaw cycles (−196 °C/10^{-2} Torr/ambient temperature) and then sealed at 10^{-2} Torr. The sample solution was irradiated through a cutoff filter ($\lambda > 360$ nm) with a 2-kW Xe lamp at 20 ± 1 °C for 6 h. After evaporation in vacuo, the product yields were determined by ^{1}H NMR analyses with an internal standard for integration. Similar photo-irradiation of **5** (94.4 mg, 0.36 mmol) and **6** (86.6 mg, 0.30 mmol) gave **17** (47.5 mg, 0.22 mmol, 61% isolated yield) and a mixture of **19** (39.8 mg, 0.22 mmol, 67%) and **20** (21.1 mg, 0.12 mmol, 70%).

Compound 20: Yellow oil. B.p. 101−102 °C at 4 Torr (ref.[18] 77−80 °C at 0.5 Torr). IR (KBr): $\tilde{\nu}$ = 1782, 1720 cm^{-1} (ref.[18] 1785, 1728 cm^{-1}). MS (EI, 70 eV): *m*/*z* (%) = 154 (8), 83 (100) [$(CH_3)_2CCH(CO)$], 55 (12). MS (CI, 15 eV): *m*/*z* (%) = 183 (23) [MH$^+$], 101 (6). ^{1}H NMR (200 MHz, $CDCl_3$): δ = 1.96 (s, 6 H), 2.23 (s, 6 H), 5.71 (br. s, 2 H) ppm. ^{13}C NMR (50 MHz, $CDCl_3$): δ = 20.74 (2 C), 27.72 (2 C), 115.26 (2 C), 162.14 (2 C), 162.94 (2 C) ppm.

Quantum Chemical Calculation: Quantum chemical calculations were performed with the aid of the programs Gaussian 98[28] and WinMOPAC 2002.[29] WinMOPAC 3.5[30] was used to draw the graphics in Figure 2. The Cartesian coordinates for **1** and **6** and the sums of calculated partial spin and charge densities for **11**$^{\cdot+}$, **14**$^{\cdot+}$, and **16** are available as Supporting Information (for Supporting Information see also the footnote on the first page of this article).

Acknowledgments

We gratefully acknowledge financial support (No. 1405008) as a Grant-in-Aid for Scientific Research on Priority Areas (Area No. 417) from the Ministry of Education, Culture, Sports, Science, and Technology of Japan.

---

[1] For recent reports on tetramethyleneethane and related systems, see: [1a] G. Maier, S. Senger, *Eur. J. Org. Chem.* **1999**, 1291−1294. [1b] K. Matsuda, H. Iwamura, *J. Am. Chem. Soc.* **1997**, *119*, 7412−7413.

[2] For the parent tetramethyleneethane radical cation, see: [2a] F. Gerson, A. de Meijere, X.-Z. Qin, *J. Am. Chem. Soc.* **1989**, *111*, 1135−1136. [2b] F. Gerson, R. Schmidlin, A. de Meijere, T. Späth, *J. Am. Chem. Soc.* **1995**, *117*, 8431−8434.

[3] For recent reports on oxyallyl and related systems, see: [3a] B. A. Hess Jr., *J. Am. Chem. Soc.* **2002**, *124*, 920−921. [3b] B. A. Hess Jr., L. Smentek, *Eur. J. Org. Chem.* **1999**, 3363−3367. [3c] A. R. Matlin, P. M. Lahti, D. Appella, A. Straumanis, S. Lin, H. Patel, K. Jin, K. P. Schrieber, J. Pauls, P. Raulerson, *J. Am. Chem. Soc.* **1999**, *121*, 2164−2173. [3d] D. A. Hrovat, M. A. Murcko, P. M. Lahti, W. T. Borden, *J. Chem. Soc., Perkin Trans. 2* **1998**, 1037−1044. [3e] T. S. Sorensen, F. Sun, *J. Chem. Soc., Perkin Trans. 2* **1998**, 1053−1062. [3f] H. J. C. Matthew, J. A. Berson, *J. Am. Chem. Soc.* **1996**, *118*, 6241−6251. [3g] D. Lim, D. A. Hrovat, W. T. Borden, W. L. Jorgensen, *J. Am. Chem. Soc.* **1994**, *116*, 3494−3499.

[4] For recent reports on tetramethylenemethane and related systems, see: [4a] H. Ikeda, K. Akiyama, Y. Takahashi, T. Nakamura, S. Ishizaki, Y. Shiratori, H. Ohaku, J. L. Goodman, A. Houmam, D. D. M. Wayner, S. Tero-Kubota, T. Miyashi, *J. Am. Chem. Soc.* **2003**, *125*, 9147−9157. [4b] H. Ikeda, T. Nakamura, T. Miyashi, J. L. Goodman, K. Akiyama, S. Tero-Kubota, A. Houmam, D. D. M. Wayner, *J. Am. Chem. Soc.* **1998**, *120*, 5832−5833. [4c] E. Nakamura, S. Yamago, *Acc. Chem. Res.* **2002**, *35*, 867−877. [4d] W. A. Russu, V. P. Villalon, V. R. Wang, J. A. Miranda, R. D. Little, *Tetrahedron Lett.* **2002**, *43*, 8459−8461. [4e] W. R. Roth, H. Wildt, A. Schlemenat, *Eur. J. Org. Chem.* **2001**, 4081−4099. [4f] A. K. Allan, G. Law Carroll, R. D. Little, *Eur. J. Org. Chem.* **1998**, 1−12.

[5] For recent reports on tetramethylenemethane-type radical cations, see: [5a] E. C. Brown, W. T. Borden, *J. Phys. Chem. A* **2002**, *106*, 2963−2969. [5b] P. K. Chou, L. Gao, S. E. Tichy, S. L. Painter, S. C. Blackstock, H. I. Kenttaemaa, *J. Phys. Chem. A.* **2000**, *104*, 5530−5534. [5c] M. Nakamura, M. Toganoh, H. Ohara, E. Nakamura, *Org. Lett.* **1999**, *1*, 7−9. [5d] H. J. P. d. Lijser, T. S. Cameron, D. R. Arnold, *Can. J. Chem.* **1997**, *75*, 1795−1809. [5e] K. Komaguchi, M. Shiotani, A. Lund, *Chem. Phys. Lett.* **1997**, *265*, 217−223. [5f] S. L. Painter, S. C. Blackstock, *J. Am. Chem. Soc.* **1995**, *117*, 1441−1442. See also refs.[4a, b]

[6] H. Ikeda, F. Tanaka, K. Akiyama, S. Tero-Kubota, T. Miyashi, *J. Am. Chem. Soc.* **2004**, *126*, 414−415

[7] P. R. Brook, J. M. Harrison, K. Hunt, *J. Chem. Soc., Chem. Commun.* **1973**, 733−734.

[8] D. Rehm, A. Weller, *Isr. J. Chem.* **1970**, *8*, 259−271.

[9] A. Weller, *Z. Phys. Chem. (Munich)* **1982**, *133*, 93−98.

[10] I. R. Gould, D. Ege, J. E. Moser, S. Farid, *J. Am. Chem. Soc.* **1990**, *112*, 4290−4301.

[11] The heats of formation of **12**$^{\cdot+}$ and **13**$^{\cdot+}$ were calculated by PM5/UHF to be +198.13 and +191.75 kcal/mol.

[12] R. Akaba, Y. Niimura, T. Fukushima, Y. Kawai, T. Tajima, T. Kuragami, A. Negishi, M. Kamata, H. Sakuragi, K. Tokumaru, *J. Am. Chem. Soc.* **1992**, *114*, 4460−4464.

[13] The absorption spectrum obtained by γ-ray irradiation of **6** in a *n*BuCl matrix at 77 K had a $\lambda_{max.}$ near 340 nm. In contrast, the 1,1-diphenylethyl radical generated by similar γ-ray irradiation of 1,1-diphenylethanol in a methylcyclohexane matrix and the 1,1-diphenylethyl cation generated by the reaction of 1,1-diphenylethanol with fluorosulfuric acid in methanol at 195 K exhibited absorptions with $\lambda_{max.}$ = 336 and 424 nm, respectively. These findings also suggest that **6** generates type A of **14**$^{\cdot+}$ on oxidation.

[14] M. A. Miranda, M. A. Izquierdo, *J. Am. Chem. Soc.* **2002**, *124*, 6532−6533.

[15] M. A. Miranda, M. A. Izquierdo, *J. Org. Chem.* **2002**, *67*, 4138−4142.

[16] M. A. Miranda, M. A. Izquierdo, *Chem. Commun.* **2003**, 364−365.

[17] C. Reichardt, in *Solvents and Solvents Effects in Organic Chemistry*, Wiley-VCH, Weinheim, **1988**, pp. 339−405.

[18] J. Cabré-Castellví, A. Palomo-Coll, A. L. Palomo-Coll, *Synthesis* **1981**, *8*, 616−620.

[19] For a recent review of methyleneketenes, see: A. E.-A. M. Gaber, H. McNab, *Synthesis* **2001**, 2059−2074.

[20] P. H. Mazzocchi, M. W. Bowen, J. Kachinsky, *J. Chem. Soc., Chem. Commun.* **1977**, 53−54.

[21] K. Mizuno, C. Pac, in *CRC Handbook of Organic Photochemistry and Photobiology* (Eds.: W. M. Horspool, P.-S. Song), CRC, New York, **1995**, pp. 358−374.

[22] D. L. Mitchell, in *CRC Handbook of Organic Photochemistry and Photobiology* (Eds.: W. M. Horspool, P.-S. Song), CRC, New York, **1995**, pp. 1326−1331.

[23] S. D. Rose, in *CRC Handbook of Organic Photochemistry and Photobiology* (Eds.: W. M. Horspool, P.-S. Song), CRC, New York, **1995**, pp. 1332−1346.

[24] N. L. Bauld, D. Gao, in *Electron Transfer in Chemistry*, vol. 2 (Ed.: V. Balzani), Wiley-VCH, Weinheim, **2001**, pp. 133−206.

[25] See references[14−16] and the references cited therein.

[26] J. K. Crandall, D. J. Keyton, J. Kohne, *J. Org. Chem.* **1968**, *33*, 3655−3657.

[27] E. C. Taylor, A. McKillop, G. H. Hawks, in *Organic Syntheses, Coll. Vol. 6*, John Wiley & Sons, New York, **1988**, p. 549−551.

[28] M. J. Frisch, G. W. Trucks, H. B. Schlegel, G. E. Scuseria, M. A. Robb, J. R. Cheeseman, V. G. Zakrzewski, J. A. Montgomery, R. E. Stratmann, J. C. Burant, S. Dapprich, J. M. Millam, A. D. Daniels, K. N. Kudin, M. C. Strain, O. Farkas, J. Tomasi, V. Barone, M. Cossi, R. Cammi, B. Mennucci, C. Pomelli, C. Adamo, S. Clifford, J. Ochterski, G. A. Petersson, P. Y. Ayala, Q. Cui, K. Morokuma, D. K. Malick, A. D. Rabuck, K. Raghavachari, J. B. Foresman, J. Cioslowski, J. V. Ortiz, B. B. Stefanov, G. Liu, A. Liashenko, P. Piskorz, I. Komaromi, R. Gomperts, R. L. Martin, D. J. Fox, T. Keith, M. A. Al-Laham, C. Y. Peng, A. Nanayakkara, C. Gonzalez, M. Challacombe, P. M. W. Gill, B. G. Johnson, W. Chen, M. W. Wong, J. L. Andres, M. Head-Gordon, E. S. Replogle, J. A. Pople, Gaussian 98 (*Revision A.11.4)*, Gaussian Inc., Pittsburgh PA, **1998**.

[29] J. J. P. Stewart, *MOPAC2002*, Fujitsu Ltd., Tokyo, Japan, **2002**.

[30] *WinMOPAC 3.5*, Fujitsu Ltd., Tokyo, Japan, **2002**.

Received November 5, 2003